Models for Tropopause Height and Radiative-Convective Equilibrium

Shineng Hu

August 16, 2015

1 Introduction

Radiative-convective equilibrium (RCE) is the equilibrium state that a convective system reaches, where convective heating compensates radiative cooling. RCE has often been used to represent the planetary atmosphere on a global scale, and it is also useful for studying the tropical climates since tropical atmosphere is always believed to reside in a near RCE state.

There is a hierarchy of numerical models that have been developed to study the RCE system, ranging from radiative-convective models (RCMs) with parameterized convection to cloud resolving models (CRMs) with explicit convective processes. Those numerical models have led us to a much deeper understanding of the radiative-convective system, but the basic physics of RCE is still far from fully understood.

One important reason is that, although the RCE concept is already simplified from reality, the full RCE system (or model) is still too complicated at least in two aspects. First, radiative and convective processes are highly coupled and nonlinear. For example, convection transports water vapor from the boundary layer to the free troposphere, and it effectively influences the absorbed longwave radiation in the atmosphere, which in turn affects the local buoyancy (temperature) and thus convection. Second, current RCMs or CRMs are usually divided into tens of vertical layers. The exchange of mass and energy between different layers makes the system very difficult to diagnose.

To better understand the RCE system, one can try to simplify either aspect above, and this is one of the motivations of this study. Accordingly, the main goal of this study is twofold. The first part will stick with multiple layers, but try to reduce the coupling of the system by specifying some variables like lapse rate and optical depth. One main goal of this part is to understand the structure of earth's tropopause by taking advantage of the simplifications we made here. The second part will try to develop a maximally simplified RCE model with an interactive hydrological cycle to better understand the basic physics of RCE itself. This model contains two layers in troposphere, but the convective and radiative processes are still highly coupled. More details will be discussed below.

2 The height of tropopause

2.1 Background

Tropopause is usually referred to as the boundary between the troposphere and the stratosphere, even though it has various definitions based on the spatial structures of temperature, potential vorticity, and chemical concentrations. Understanding the height of tropopause is important to studying the column total ozone [1] and also the mass exchange between the troposphere and the stratosphere [2].

Despite its importance, many problems related to the observed features of the tropopause remain unsolved. From observations, the height of tropopause is higher in the tropics (16km) and lower in the polar regions (8km), and this transition sharply occurs in the mid-latitudes (Fig. 1a). What shapes this particular structure? Also, tropical tropopause, compared with the one in extratropics, is not only higher, but also colder and sharper (Fig. 1b). What can explain those three features simultaneously?

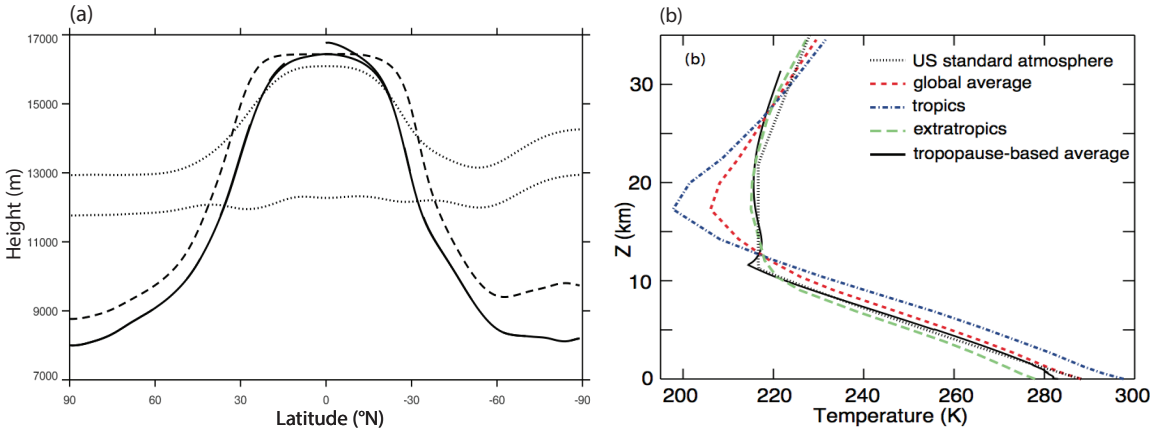

Figure 1: (a) Zonal-mean tropopause height as a function of latitude (solid). Figure adopted from [3]. (b) Zonal mean temperature profiles in different regions. Note the contrast between tropics (blue dash-dotted) and extratropics (green dashed). Figure adopted from [4].

To that end, we will use a extremely simplified tropopause model, and see whether this one-dimensional (1-D) model can reproduce the observed structure of tropopause. One thing noteworthy is that there will be no explicit dynamics in this model, although lateral transport and mid-latitude eddies are shown to be important in shaping the tropopause structure. Our following results will show that the observed features of tropopause can be surprisingly well captured by this simple 1-D model.

2.2 Numerical model

Let's start with a two-stream grey atmosphere, which is commonly used in early related studies [5, 6], and write the radiation transfer equation for longwave radiation as,

$$\frac{\partial D}{\partial \tau} = B - D, \qquad \frac{\partial U}{\partial \tau} = U - B, \tag{2.1}$$

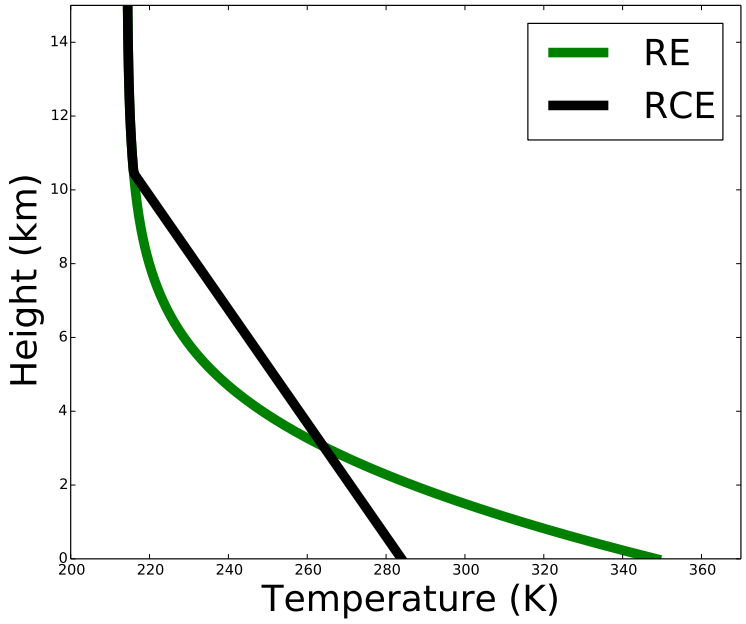

Figure 2: Temperature profiles for radiative equilibrium (green) and radiative-convective equilibrium (black).

where D and U are downward and upward longwave radiation, $B = \sigma T^4$ is Stefan-Boltzmann law, and τ is optical depth increasing downward. Then we can quickly rewrite Eq. (2.1) as

$$\frac{\partial I}{\partial \tau} = J - 2B, \qquad \frac{\partial J}{\partial \tau} = I \tag{2.2}$$

using

$$I = U - D, \qquad J = U + D. \tag{2.3}$$

Consider a radiative equilibrium (RE) state and assume that no shortwave radiation is absorbed by the atmosphere, then the convergence of net longwave radiation should vanish, which can be expressed as,

$$\frac{\partial I}{\partial \tau} = 0. \tag{2.4}$$

Furthermore, by using the boundary condition at the top of the atmosphere,

$$\tau = 0 : \qquad U = U_t = \sigma T_e^4, \quad D = 0 \tag{2.5}$$

we arrive at the solutions for radiative equilibrium,

$$D(\tau), U(\tau), B(\tau) = \left(\frac{\tau}{2}, \frac{\tau + 2}{2}, \frac{\tau + 1}{2} \right) U_t. \tag{2.6}$$

The temperature profile from this solution is shown as the green line in Fig. 2

Let's look at several features of RE solutions. When τ is very small, B/U is one half, and it physically means that near the top of the atmosphere, half of upward longwave radiation is coming from remote radiative transfer. Note that, until now, we have not used any boundary condition at the surface. So this observation will be valid for any cases with any lower boundary conditions, as long as the upper atmosphere is in the radiative equilibrium state; it will be used in the following analysis when we are deriving the analytical approximation of RCE solutions. Now consider at the surface, the difference between U and B is always non-zero. It indicates that there is always a temperature jump between ground temperature and near-surface air temperature in RE solutions, and this temperature jump is actually nontrivial, around $10K$. Another main feature is that the lapse rate near the surface is so high that convection can occur, which will result in a new equilibrium state called radiative-convective equilibrium (RCE) state.

Within this new equilibrium state, the system is in RE in the stratosphere, given by the solutions above, while in RCE in the troposphere with a uniform lapse rate. Mathematically, the temperature profile can be expressed as,

$$T(z) = \begin{cases} T_{re}, & z \geq H_T, \\ T_T + \Gamma(H_T - z), & H_T \geq z \geq 0, \end{cases} \tag{2.7}$$

where H_T is the tropopause height, and T_T is the tropopause temperature. The two vertical coordinates (τ and z) can be related by the formulation below,

$$\tau(z) = \tau_s \left[f_{H_2O} exp(-z/H_a) + (1 - f_{H_2O}) exp(-z/H_s) \right] \tag{2.8}$$

where τ_s is surface optical depth, f_{H_2O} is a linear parameter controlling the contribution of water vapor to optical depth compared with carbon dioxide, H_a is the scale height of water vapor (typically 2km), and H_s is the scale height of carbon dioxide (typically 8km). Additionally, we should add one more boundary condition at the surface,

$$\tau = \tau_s : \qquad U = B = \sigma T_s^4. \tag{2.9}$$

We can solve this set of equations numerically by integrating Eq. (2.1) from the top of the atmosphere to the surface given a certain H_T, and iterate the calculation to match both boundary conditions. The temperature profile associated with the RCE solutions is shown as the black curve in Fig. 2.

Note that the RCE solution above is a function of emission temperature T_e, surface optical depth τ_s, and tropospheric lapse rate Γ. The sensitivity of tropopause height to those three parameters are presented in Fig. 3. Tropopause height significantly increases when surface optical depth increases or tropospheric lapse rate decreases; tropopause height increases with outgoing longwave radiation but its impact is not as strong as the other two parameters.

2.3 Analytical approximation

To better understand the phase diagrams in Fig. 3, it is helpful to derive an analytical expression for tropopause height. However, finding the exact analytical solution is very difficult due to the multiple-layer model set-up and the nonlinearity of the system. Therefore,

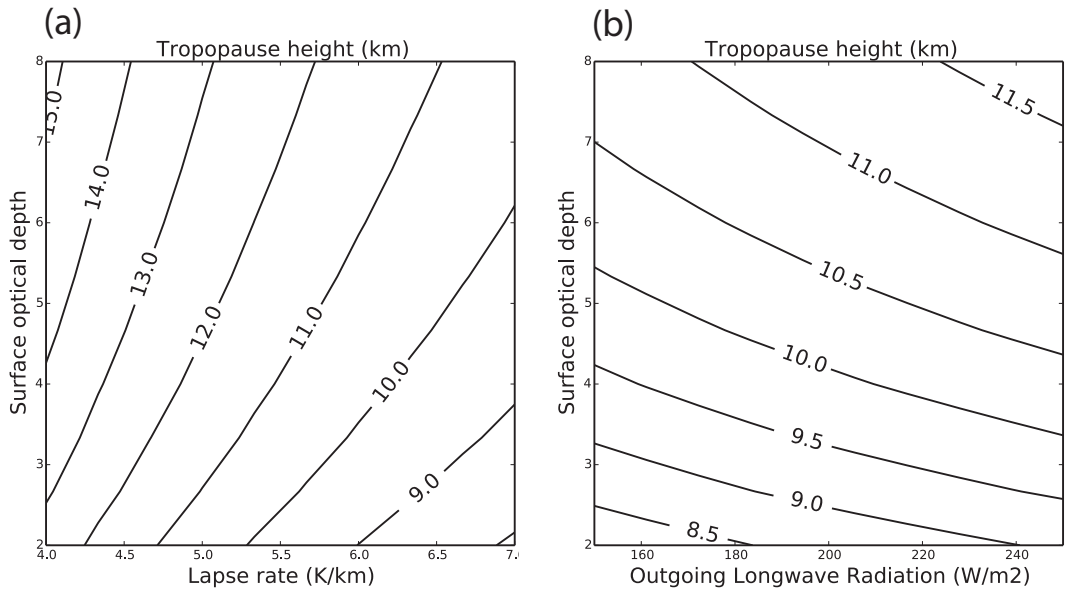

Figure 3: Tropopause height as a function of surface optical depth and (a) tropospheric lapse rate and (b) outgoing longwave radiation. Note that the parameter ranges are chosen as typical ranges of earth's atmosphere.

we make the following assumptions. First, temperatures above the tropopause are uniform and equal to $2^{-1/4}T_e$, which is obtained from Eq. (2.6) by simply setting τ to be zero. Second, as mentioned before, the lapse rate is held uniform throughout the whole troposphere below H_T. Third, the contribution to optical depth all comes from water vapor, that is, f_{H_2O} is set to 1. Fourth, B/U linearly increases from 1/2 (radiative equilibrium when τ is zero) at the tropopause to 1 (lower boundary condition) at the surface, which can be expressed as $B/U = 1 - z/2H_T$, and this assumption is fairly good for a wide range of surface optical depth and tropospheric lapse rate as shown in Fig. 4.

With those assumptions, we can eventually derive an analytical approximation for the height of tropopause as follows,

$$H_T = \frac{1}{16\Gamma}\left(CT_T + \sqrt{C^2T_T^2 + 32\Gamma\tau_s H_a T_T}\right), \tag{2.10}$$

where $C = ln4 \approx 1.38$. This expression agrees quite well with the sensitivity results presented in Fig. 3.

2.4 What shapes the observed tropopause structure from an RCE perspective? The role of Brewer-Dobson circulation

One question we can ask is could we reproduce the observed tropopause structure using this 1-D RCE model? To this end, we should first get the observed latitude dependence of lapse rate, optical depth, and outgoing longwave radiation, and then plug them into this simple model. We will go through those three parameters as inputs one by one, and only the zonal-mean annual-mean results will be discussed.

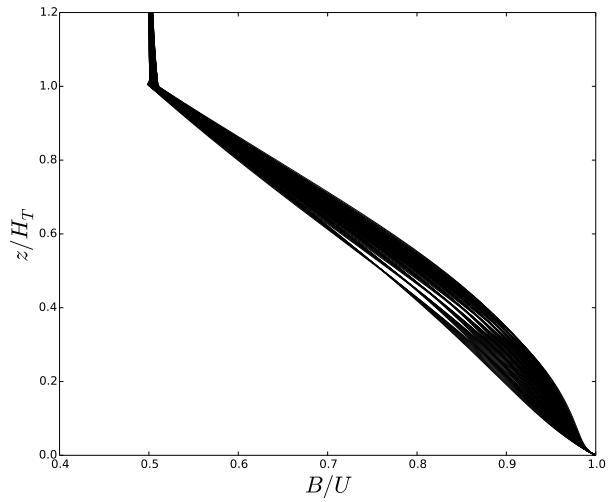

Figure 4: Validation of the assumption $B/U = 1 - z/2H_T$ for different combinations of surface optical depth and tropospheric lapse rate.

Tropospheric lapse rate decreases from $6.5K/km$ in the tropics to $4K/km$ in the polar regions [7, 8]. In the tropics, deep moist convection makes the lapse rate very close to the moist adiabatic lapse rate. However, in the polar regions, it is noteworthy that the lapse rate is not controlled by dry adiabatic lapse rate (about $9.8K/km$); instead, the value of $4K/km$ is determined by the critical lapse rate that satisfies the condition of baroclinic adjustments [7]. Surprisingly, the structure of lapse rate leads to an increase in the tropopause height from the tropics to polar regions by over 3km, which is opposite to the observed structure (blue line in Fig. 6).

As water vapor concentration decreases dramatically from tropics to polar regions, surface optical depth also decreases significantly. In this model, we are using a grey atmosphere; therefore, getting the observed equivalent surface optical depth is not very straightforward. An alternative way is to use the optical depth structure used in idealized GCMs. Following previous studies [9, 10], we will let the surface optical depth change sinusoidally from 7.2 in tropics to 1.8 in polar regions and set the parameter f_{H_2O} to 0.8. As a result, tropopause height decreases from tropics to polar regions by about 3km, which almost totally compensates the effect of optical depth (magenta line in Fig. 6).

Concerning the outgoing longwave radiation, it tends to yield a higher tropopause in the tropics, but as we mentioned above, its impact is very limited (red line in Fig. 6).

Combining all three effects, we will get an almost uniform tropopause height, about 10.5km, across different latitudes (black solid line in Fig. 6). Its pattern indeed mimics the observed pattern: higher in the tropics and lower in the polar regions with sharp changes occurring in the mid-latitudes. However, the tropical tropopause is only about 0.5km higher than the polar tropopause, which is much smaller than the observed value 8km. What might be missing?

Brewer-Dobson circulation in the stratosphere can cause the adiabatic heating (or cool-

ing) locally near the tropopause, therefore it can potentially change the height of tropopause. The heating rate is essentially determined by vertical velocity and thermal stratification,

$$\frac{\partial \theta}{\partial t} = -w\frac{\partial \theta}{\partial z} = Q_s. \tag{2.11}$$

From observations, the vertical gradient of potential temperature is positive all around the globe. So the ascents (descents) in the tropical (polar) stratosphere will induce a local adiabatic cooling (heating). Rough estimates from observations $w \approx 0.3mm/s, \partial\theta/\partial z \approx 40K/km$, give us a heating rate of $Q_s \approx 1K/day$. Due to this additional adiabatic heating, we need to rewrite the radiative equilibrium condition Eq. (2.4) as

$$\frac{\partial I}{\partial z} = \rho c_p Q_s, \tag{2.12}$$

where ρ is the density of air and c_p is the heat capacity of air.

After imposing the heating structure shown in the lower-right panel of Fig. 5, we can get a structure of tropopause height (thick green line in Fig. 6) very like observations (black solid line in Fig. 1a). The adiabatic cooling significantly raises the tropical tropopause by 3km, and the adiabatic heating also lowers the polar tropopause by 1km. Eventually we get a tropopause with very similar structure as observations in both the general pattern and the equator-pole contrast.

Brewer-Dobson circulation not only raises the tropical tropopause, but also makes it colder and sharper, which otherwise cannot be explained by any of the three parameters (Fig. 7a,b). Comparing our results (Fig. 7b) and the observations (Fig. 1b), we find that our model, in spite of its simplicity, well captures all three main features of tropical tropopause: higher, colder, and sharper than the extratropical tropopause. By adding ozone heating in the upper troposphere, we can get an even more realistic temperature profile (Fig. 7c) compared to observations (Fig. 1b).

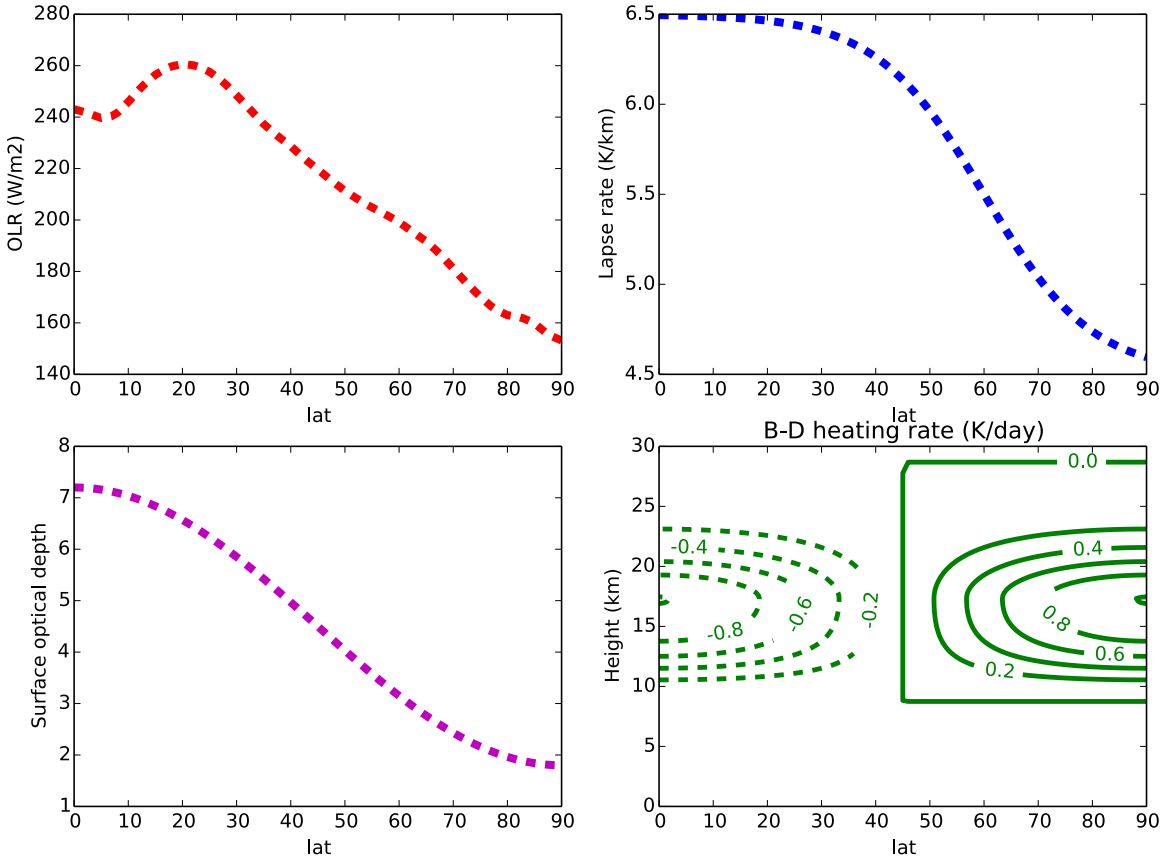

Figure 5: Meridional structure of outgoing longwave radiation, tropospheric lapse rate, surface optical depth, and adiabatic heating rate by Brewer-Dobson circulation, which have been used as inputs in the 1-D tropopause model. OLR is computed from NOAA OLR dataset. Lapse rate is a best-fit tangent curve to observed values. Surface optical depth is following the previous study with idealized GCMs. Adiabatic heating rates are artificially imposed just above the tropopause.

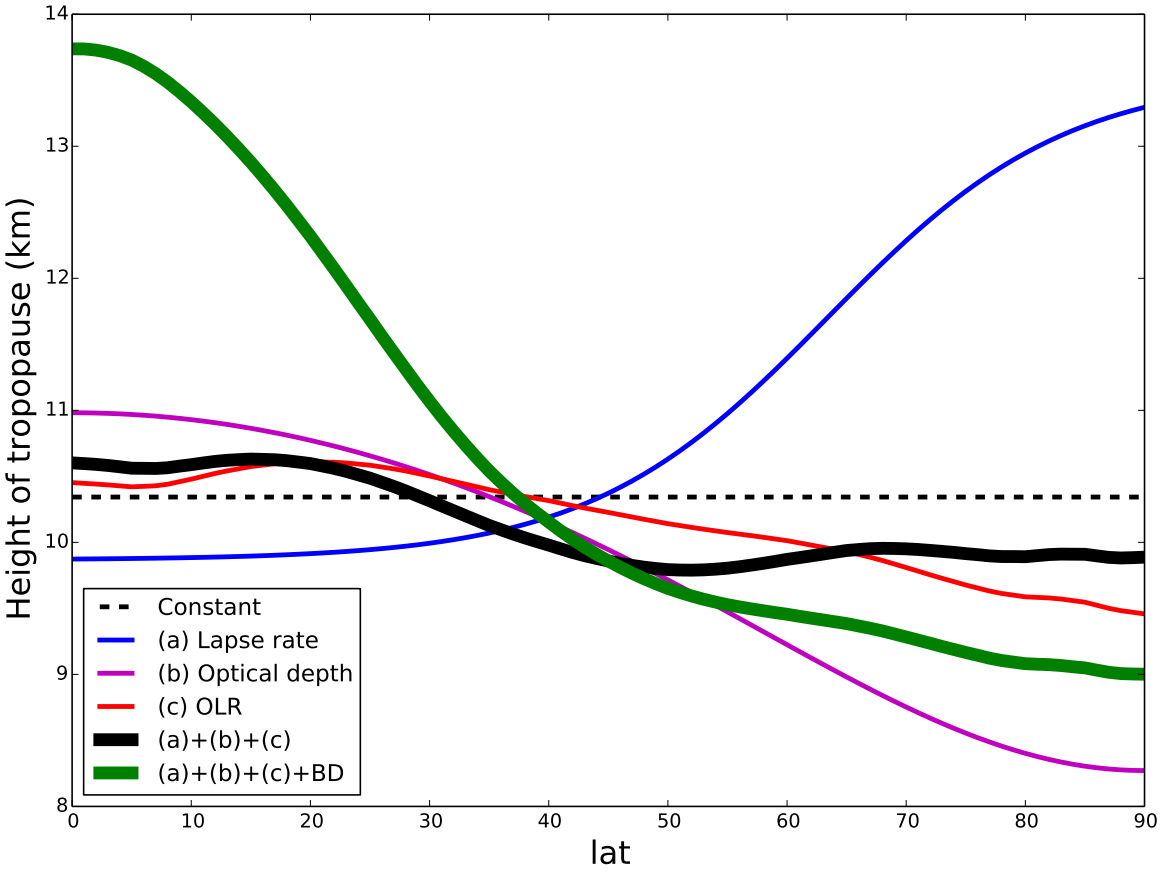

Figure 6: Meridional structure of tropopause height from the numerical solutions of 1-D tropopause model. The black dashed line is with all parameters constant. Three thin color lines are with only lapse rate (blue), optical depth (magenta), or OLR (red) changing with latitude. The thick black solid line is with all three parameters changing with latitude. The thick green solid line is with all three parameters changing with latitude and also an imposed adiabatic heating by Brewer-Dobson circulation.

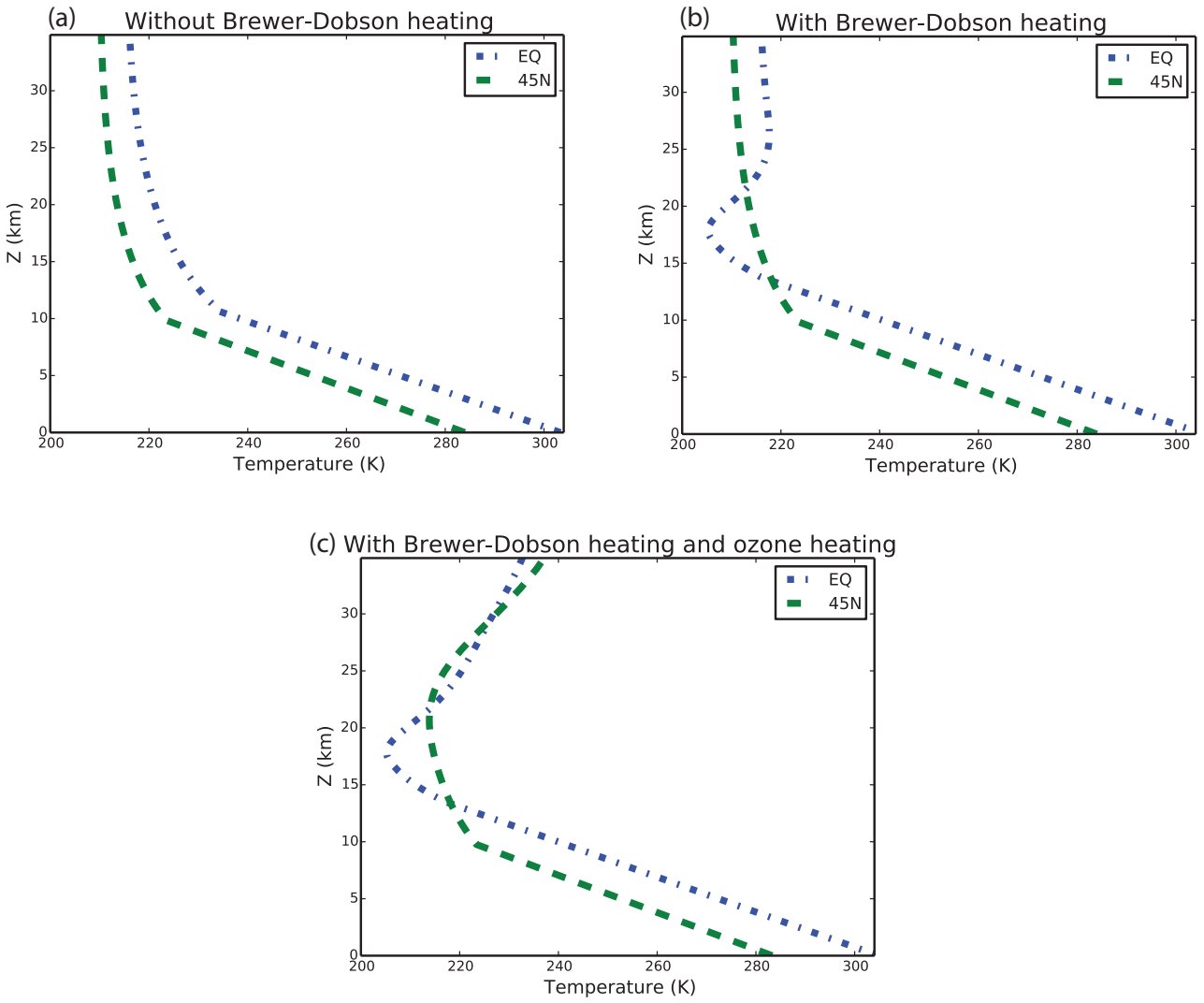

Figure 7: The contrast of temperature profiles at equator and $45^o N$. (a) With all three parameters changing with latitude, (b) adding adiabatic heating (Brewer-Dobson circulation) onto case a, and (c) adding both adiabatic heating (Brewer-Dobson circulation) and diabetic heating (ozone) onto case a.

3 A two-layer RCE model

3.1 Background

In the tropopause model we just talked about, radiation and convection are two separate processes. Radiation accounts for the energy balance of the system, while convection acts to set the tropospheric lapse rate. In reality, the two processes are highly coupled. There are quite a few RCE studies with highly coupled models, such as radiative-convective models (RCMs) and cloud resolving models (CRMs), but they are too complicated to help us understand the principle physics of RCE states. For example, how does relative humidity change with climates in RCE states? It involves too many elements and layers. We will develop a maximally simplified radiative-convective equilibrium (RCE) model but still with an interactive hydrological cycle, and our main goal is to answer some basic questions related to RCE like the one about relative humidity we just mentioned.

3.2 Model set-up

Following a recent study [11], the RCE model has two equal-mass layers for troposphere, and its hydrological cycle is interactive. Here we only care about the equilibrium state, instead of the stability of the state. Effective emission temperature T_e is specified, and two other parameters are the precipitation efficiency ϵ_p and the surface wind V. All the other variables, including temperature, humidity, convective mass flux, tropopause height, and heating rate are calculated.

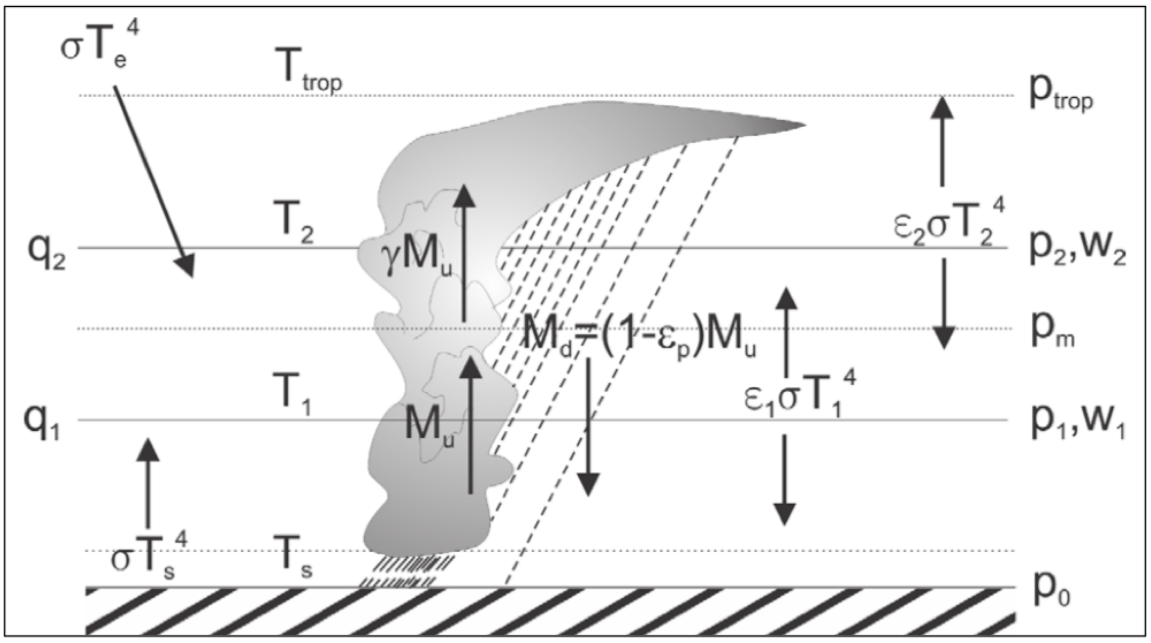

Figure 8: The schematic of the two-layer RCE model.

The basic model setup is shown in the schematic of Fig. 8. Surface pressure p_0 is specified, and the tropopause temperature is assumed to be $2^{-1/4}T_e$ as discussed in the

previous section. In the following discussions, the subscripts '1', '2', 's', 'b', 'm', and 'trop' stand for the lower layer, upper layer, surface, boundary layer, middle of troposphere, and tropopause, respectively. Note that 'middle' indicates the mid-level in terms of mass – in other words, in the pressure coordinate.

Let's start with the energy balance in the two layers. In the lower layer,

$$F_s - M_u(h_b - h_m) + Q_1 = 0, \tag{3.1}$$

where F_s is the surface turbulent enthalpy flux, M_u is the convective mass flux, h_b and h_m is the moist static energy (MSE) in the middle of troposphere and in the subcloud layer, and Q_1 is the radiative cooling. Surface turbulent enthalpy flux is essentially determined by surface wind speed, surface saturation specific humidity, and surface relative humidity,

$$F_s = \tilde{V}(h_s - h_b) \approx \tilde{V} L_v q_s^* (1 - \mathcal{H}_s), \tag{3.2}$$

where $\tilde{V}$ is defined as

$$\tilde{V} = \rho_b C_k V. \tag{3.3}$$

Similarly, in the upper layer,

$$M_u(h_b - h_m) + Q_2 = 0, \tag{3.4}$$

where we assume the MSE at the tropopause is the same as that in the subcloud layer, so there is no MSE exchange at the tropopause.

Energy balance should also hold in the clear air between clouds. In the lower layer, assuming convective downdraft as $(1 - \epsilon_p)M_u$, we can have that the large-scale subsidence in the clear air is $\epsilon_p M_u$. So the energy balance can be written as

$$\epsilon_p M_u \Delta S_1 + Q_1 = 0, \tag{3.5}$$

where we are assuming convection only occupies a very small portion of the domain area, and ΔS_1 is the contrast in dry static energy between the mid-troposphere and the surface,

$$\Delta S_1 = c_p(T_m - T_s) + g z_m. \tag{3.6}$$

Similarly, we can write the energy balance in the clear air of upper layer as,

$$\gamma M_u \Delta S_2 + Q_2 = 0, \tag{3.7}$$

where ΔS_2 is the contrast in dry static energy between the tropopause and the mid-troposphere,

$$\Delta S_2 = c_p(T_{trop} - T_m) + g(z_{trop} - z_m). \tag{3.8}$$

Note that here γ, not like ϵ_p, is calculated instead of specified, so it is not a parameter.

Finally let's consider the energy balance in the subcloud layer and at the surface. In the subcloud layer, surface turbulent enthalpy flux is balanced by the convective flux out of the layer and the flux due to shallow convection; that is,

$$M_u(h_b - h_m) + F_{shallow} = F_s. \tag{3.9}$$

If we parameterize $F_{shallow}$ as $(1-\alpha)F_s$, we can then get

$$M_u(h_b - h_m) = \alpha F_s. \tag{3.10}$$

Note that here α is calculated, not a parameter. The surface energy balance requires that

$$F_s - Q_s = 0. \tag{3.11}$$

The radiative heating rates in the lower layer, the upper layer, and at the surface can be defined as,

$$Q_1 = \sigma\varepsilon_1(T_s^4 - 2T_1^4 + \varepsilon_2 T_2^4), \tag{3.12}$$

$$Q_2 = \sigma\varepsilon_2[(1-\varepsilon_1)T_s^4 - 2T_2^4 + \varepsilon_1 T_1^4], \tag{3.13}$$

$$Q_s = \sigma[T_e^4 + \varepsilon_1 T_1^4 + \varepsilon_2(1-\varepsilon_1)T_2^4 - T_s^4]. \tag{3.14}$$

In addition to those three sets of energy balance equations, we also need to make assumptions of conserved saturation MSE and saturation entropy in the whole column, which are controlled by subcloud properties. Mathematically, it can be expressed as,

$$h_b = h_1^* = h_m^* = h_2^* = h_{trop}^* \tag{3.15}$$

and

$$s_b = s_1^* = s_m^* = s_2^* = s_{trop}^*. \tag{3.16}$$

Since this is a highly coupled and nonlinear system, we need to solve it numerically. Numerical solutions will be discussed in the following subsections.

3.3 State-dependent emissivity

Before we talk about the solutions, one thing we want to emphasize is the state-dependence of layer emissivities. Intuitively, we can imagine that when water vapor increases in a certain layer, more longwave radiation can be absorbed or emitted given a certain temperature; in other words, layer emissivity will increase. But, quantitively determining the relationship between emissivity and water vapor (or temperature) is not a trivial problem. As a first step, we can try to use an artificial exponential function to mimic the Clausius-Clapeyron relation, but the parameters we will choose are quite empirical. We notice that this relation is a key element coupling radiation and convection, so it will largely affect the model behavior. Thus, we decide to use more realistic formulation to get a more reasonable model behavior.

Following a very early study [12], we seek to find a relation between layer emissivity and water vapor path (WVP, sometimes also called total precipitable water, defined as the height of water if all water vapor in a certain layer condenses to liquid water). Carbon dioxide has been taken into account, but its concentration is held as constant around 400ppmv. The overlap of absorption spectrum between water vapor and carbon dioxide has also been corrected. Results are shown in Fig. 9. The WVP of current earth is about 27mm, ranging from 1mm in the polar regions to 42mm in the tropics, so the layer emissivity is roughly in the range of 0.6 to 0.8.

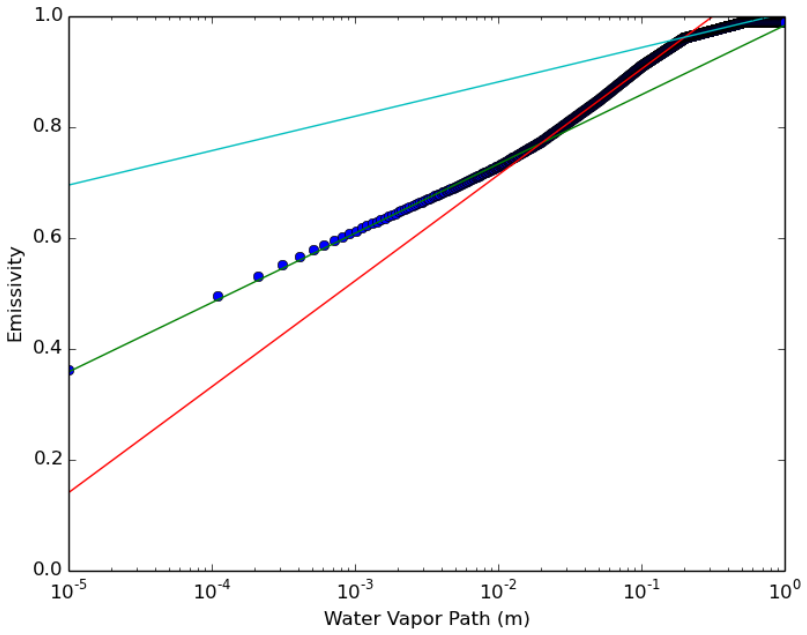

Figure 9: Relation between layer emissivity and water vapor path, with the best-fit lines in different ranges of water vapor path [12].

3.4 General behaviors of the two-layer RCE model

In general, our two-layer model well captures most important features of an RCE system, but here we will just discuss two examples about how the model behaves. The first thing we need to check is the lapse rate. By definition, the lapse rate can be computed as the temperature contrast between the top and the bottom of a layer divided by the layer thickness. Then we can compare this value with the theoretical value of moist adiabatic lapse rate, which can be computed with the average layer temperature. In principle, those two values should be approximately the same, and this feature is well captured by our two-layer model as expected (Fig. 10).

Another example we want to show is how convection strength changes with climates. Recall that Eq. (3.4) basically states that in the second layer, radiative cooling balances the convective heating, which is determined by both convective mass flux and the MSE contrast between the mid-troposphere and the tropopause (note that $h_b = h^*_{trop} = h_{trop}$ because the tropopause is extremely dry). When SST increases, on one hand, radiative cooling will increase because both temperature and emissivity increase; on the other hand, the MSE contrast also increases because the satiation specific humidity increases significantly with temperature following Clausius-Clapeyron relation. In comparison, the MSE contrast increases much faster than the radiative cooling, so the convective mass flux will decrease, as is seen from the full cloud resolving simulations (Fig. 11b). This feature is also captured by our two-layer model (Fig. 11a). Note that here we are focused on RCE states, and things will be different if one considers weak temperature gradient (WTG) simulations.

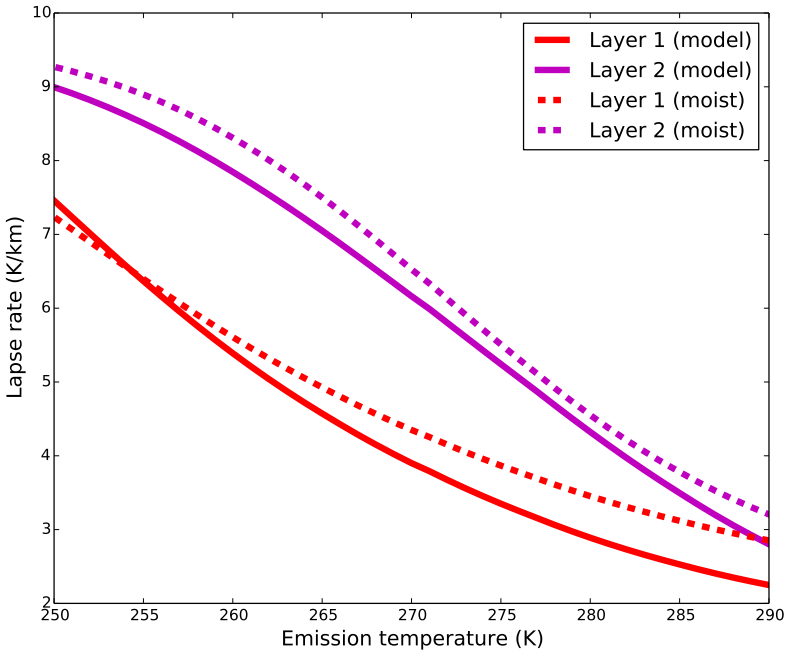

Figure 10: Comparison of the model lapse rate and the theoretical moist adiabatic lapse rate in both layers for different emission temperatures.

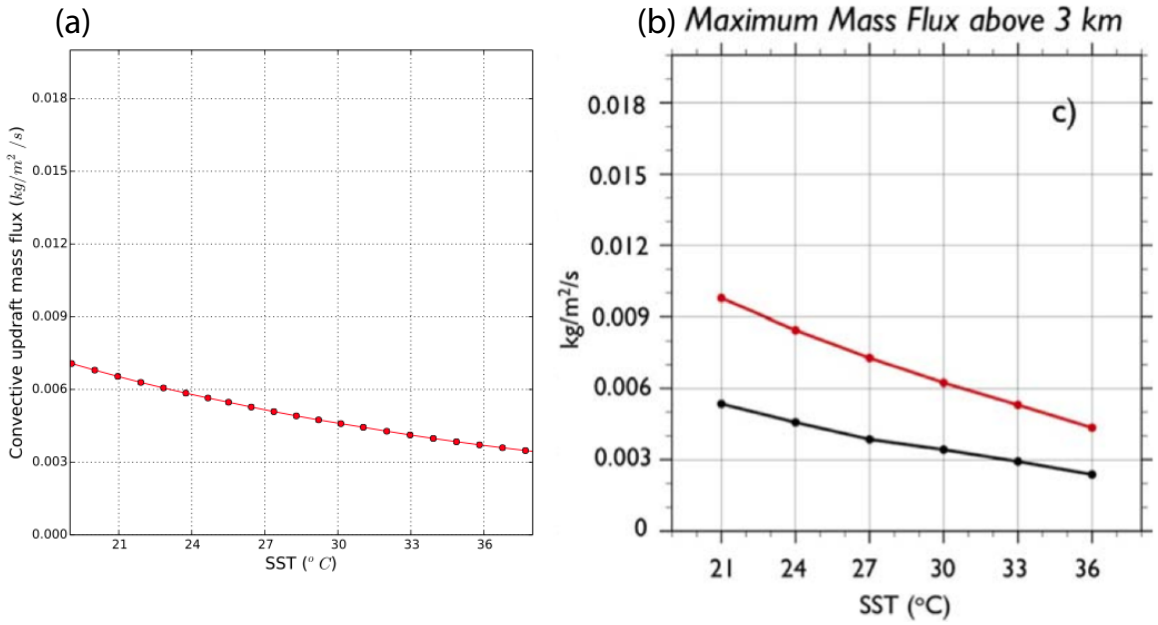

Figure 11: Comparison of (a) the convective mass flux (in the lower layer) from our two-layer model and (b) the maximum convective mass flux (red line) from a cloud resolving model [13].

3.5 How does relative humidity change with climates from an RCE perspective?

How relative humidity changes with climates is a fundamental and important question, but we still lack a complete answer to that. Some studies regard it as a constant variable in climate models, but this assumption still needs to be justified. Among all arguments related to this question, large-scale circulation argument might be known and accepted by most people in the community. It basically states that large-scale circulation transports a saturated air parcel to a warmer place, which makes it under-saturated, and the relative humidity is simply determined by the temperature difference between two places; therefore as long as the large-scale circulation does't change too much, global (or tropical) average relative humidity in the troposphere might not be able to change too much. Here we will focus on RCE states without any large-scale circulation, and our results suggest that even in RCE states, tropospheric relative humidity can not change much and a key element is the radiation-convection coupling.

Seen from our two-layer model results, tropospheric relative humidity hardly changes within a broad range of SST. When SST increases from 10^oC to 40^oC, surface relative humidity slowly increases from 0.7 to 0.9; however, the relative humidity in the free troposphere changes little and sits at a value of 0.5. To better understand this behavior, we will make use of the energy balance equations mentioned above and conduct energetics analysis.

Let's start with the surface relative humidity. From Eq. (3.2), we can easily get

$$\frac{1}{F_s}\frac{\partial F_s}{\partial T_s} = \frac{1}{q_s^*}\frac{\partial q_s^*}{\partial T_s} - \left(\frac{\mathcal{H}_s}{1-\mathcal{H}_s}\right)\frac{1}{\mathcal{H}_s}\frac{\partial \mathcal{H}_s}{\partial T_s}, \tag{3.17}$$

Similarly, from Eq. (3.14), we can get

$$\frac{1}{Q_s}\frac{\partial Q_s}{\partial T_s} = \frac{A+B}{C}, \tag{3.18}$$

where

$$\begin{aligned} A &= 4[T_e^3\frac{\partial T_e}{\partial T_s} + \varepsilon_1 T_1^3\frac{\partial T_1}{\partial T_s} + \varepsilon_2(1-\varepsilon_1)T_2^3\frac{\partial T_2}{\partial T_s} - T_s^3], \\ B &= \frac{\partial \varepsilon_1}{\partial T_s}T_1^4 + [(1-\varepsilon_1)\frac{\partial \varepsilon_2}{\partial T_s} - \varepsilon_2\frac{\partial \varepsilon_1}{\partial T_s}]T_2^4, \\ C &= T_e^4 + \varepsilon_1 T_1^4 + \varepsilon_2(1-\varepsilon_1)T_2^4 - T_s^4. \end{aligned} \tag{3.19}$$

Since layer emissivity is close to 1, the second term B/C is relatively small compared with A/C and can be neglected. Then we can simplify Eq. (3.18) as

$$\frac{1}{Q_s}\frac{\partial Q_s}{\partial T_s} \approx \frac{4}{\bar{T}}\frac{\partial \bar{T}}{\partial T_s} \approx \frac{8}{\bar{T}} \tag{3.20}$$

where $\bar{T}$ is the average tropospheric temperature, and it is roughly $280K$ when surface temperature is $300K$. The second approximation is because the value of $\partial\bar{T}/\partial T_s$ can be assumed to be 2, which indicates that, given a certain increase in surface temperature, tropospheric temperature is amplified by a factor of 2 due to the lapse rate feedback. Then

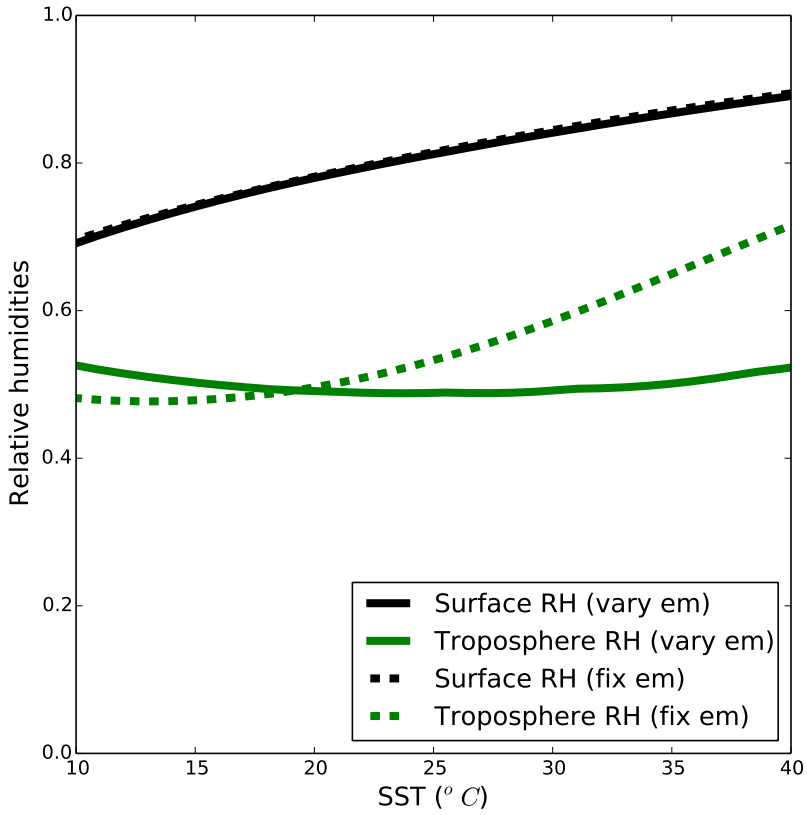

Figure 12: Surface relative humidity (black) and tropospheric relative humidity (green) as a function of sea surface temperature for the cases with varying emissivity (solid) and fixed emissivity (dashed). Note the unchanged tropospheric relative humidity for the case of varying emissivity.

combining Eq. (3.17) and Eq. (3.20), and recalling the surface energy balance Eq. (3.11), we can eventually arrive at,

$$\begin{aligned} \frac{1}{\mathcal{H}_s}\frac{\partial \mathcal{H}_s}{\partial T_s} &\approx \left(\frac{1-\mathcal{H}_s}{\mathcal{H}_s}\right)\left(\frac{1}{q_s^*}\frac{\partial q_s^*}{\partial T_s} - \frac{8}{\bar{T}}\right) \\ &\approx \left(\frac{0.18}{0.82}\right)\left(\frac{6.2\%}{1K} - \frac{8}{280K}\right) \\ &\approx 0.7\%/K, \end{aligned} \tag{3.21}$$

which is a good estimate to the black solid line in Fig. 12.

With a similar method, we can get how tropospheric relative humidity changes with SST. Combining Eqs. (3.4)(3.5), we can get

$$h_b - h_m = \epsilon_p \Delta S_1 Q_2 / Q_1, \tag{3.22}$$

and thus

$$\frac{1}{h_b - h_m}\frac{\partial(h_b - h_m)}{\partial T_s} = \frac{1}{Q_2}\frac{\partial Q_2}{\partial T_s} - \frac{1}{Q_1}\frac{\partial Q_1}{\partial T_s} + \frac{1}{\Delta S_1}\frac{\partial \Delta S_1}{\partial T_s}. \tag{3.23}$$

Then we rewrite $(h_b - h_m)$ as

$$h_b - h_m = h_m^* - h_m = L_v q_m^*(1 - \mathcal{H}_m). \tag{3.24}$$

Also, we rewrite ΔS_1 as

$$\Delta S_1 = (h_m^* - L_v q_m^*) - (h_b - L_v q_s) = L_v(q_s^* \mathcal{H}_s - q_m^*). \tag{3.25}$$

Substituting Eqs.(3.24)(3.25) into Eq.(3.23), we get

$$\frac{1}{\mathcal{H}_m}\frac{\partial \mathcal{H}_m}{\partial T_s} = \left(\frac{1 - \mathcal{H}_m}{\mathcal{H}_m}\right)\left[\frac{1}{q_m^*}\frac{\partial q_m^*}{\partial T_s} - \frac{1}{q_s^*\mathcal{H}_s - q_m^*}\frac{\partial(q_s^*\mathcal{H}_s - q_m^*)}{\partial T_s} + \frac{1}{Q_1}\frac{\partial Q_1}{\partial T_s} - \frac{1}{Q_2}\frac{\partial Q_2}{\partial T_s}\right] \tag{3.26}$$

When layer emissivity varies with SST (or WVP), the three terms in Eq. (3.26) are

$$\frac{1}{q_m^*}\frac{\partial q_m^*}{\partial T_s} \approx 9.4\%/K, \tag{3.27}$$

$$-\frac{1}{q_s^*\mathcal{H}_s - q_m^*}\frac{\partial(q_s^*\mathcal{H}_s - q_m^*)}{\partial T_s} \approx -4.4\%/K, \tag{3.28}$$

$$\frac{1}{Q_1}\frac{\partial Q_1}{\partial T_s} - \frac{1}{Q_2}\frac{\partial Q_2}{\partial T_s} \approx -5.0\%/K, \tag{3.29}$$

which are the values when SST is 300K. Substituting Eqs.(3.27)(3.28)(3.29) into Eq.(3.26), we get

$$\frac{1}{\mathcal{H}_m}\frac{\partial \mathcal{H}_m}{\partial T_s} \approx 0.0\%/K. \tag{3.30}$$

That is why tropospheric relative humidity changes little with a broad range of climate with SST varying from 10^oC to 40^oC.

Since this RCE system is highly coupled, it is hard to say which single element in this coupled system causes the almost constant tropospheric relative humidity. Actually, it is due to the radiation-convection coupling itself, in other words, the feedback between radiation and convection. To test this hypothesis, we can fix the layer emissivity to a constant value, which kills the coupling between convection and radiation, and see how the relative humidity changes with SST.

Interestingly, we find that the case with fixed emissivity experiences a significant increase in the tropospheric relative humidity with SST. This can be partly explained by the same energetics analysis we conducted above, and the new values of the three terms in Eq. (3.26) are

$$\frac{1}{q_m^*}\frac{\partial q_m^*}{\partial T_s} \approx 9.4\%/K, \tag{3.31}$$

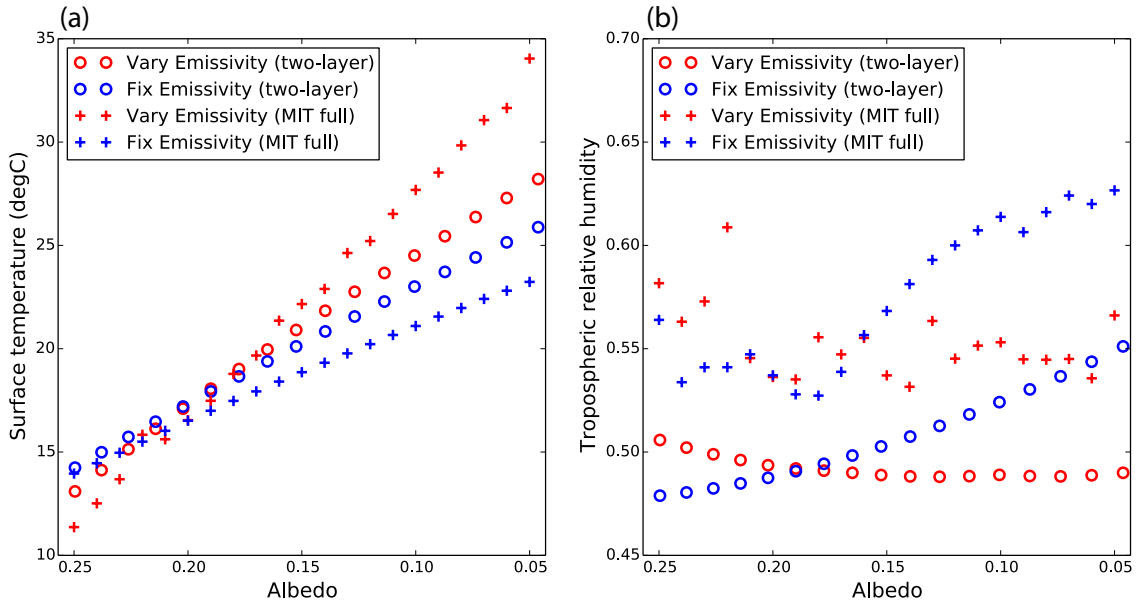

Figure 13: Comparison of (a) surface temperature and (b) tropospheric relative humidity between our two-layer model (circle) and the MIT full radiative-convective model (cross). Horizontal axis has been changed to albedo for the ease of comparison.

$$-\frac{1}{q_s^*\mathcal{H}_s - q_m^*}\frac{\partial(q_s^*\mathcal{H}_s - q_m^*)}{\partial T_s} \approx -4.1\%/K, \tag{3.32}$$

$$\frac{1}{Q_1}\frac{\partial Q_1}{\partial T_s} - \frac{1}{Q_2}\frac{\partial Q_2}{\partial T_s} \approx -2.9\%/K. \tag{3.33}$$

Again, they are the values when SST is 300K. Substituting Eqs.(3.31)(3.32)(3.33) into Eq.(3.26) and taking $\mathcal{H}_m$ as 0.55, we get

$$\frac{1}{\mathcal{H}_m}\frac{\partial \mathcal{H}_m}{\partial T_s} \approx 2.0\%/K, \tag{3.34}$$

which is a good estimate for the green dashed line in Fig. 12.

One might have noticed that fixing the layer emissivity will not change the behavior of surface relative humidity too much (black dashed line in Fig. 12). That is because the state dependency of emissivity only enters the term B in Eq. (3.19), and as we have mentioned, B is a small term and it will not change the results too much in two cases.

To further test our hypothesis about the stabilizing effect of radiation-convection coupling on the tropospheric relative humidity, we have also used a full radiative-convective model (MIT column RCM) and the results are shown in Fig. 13. In the MIT full RCM, we can modify surface albedo to change the external forcing, so for the ease of comparison, we use surface albedo as horizontal axes in Fig. 13. For the cases with varying emissivity (red), both models exhibit an almost unchanged relative humidity; for the cases with fixed emissivity (blue), both models exhibit increasing relative humidity when the system gets

warmer. Those trends agree especially well when albedo is in the range of 0.05 to 0.20, and surface temperature is in the range of 15^oC to 30^oC, which is exactly the temperature range of current tropics.

4 Conclusions and discussions

This study develops two idealized models with different simplifications from the full radiative-convective equilibrium system. The first model is a one-dimensional tropopause model with multiple layers but less coupling. We find that this 1-D model, even without any explicit dynamics, can well reproduce the observed meridional structure of tropopause height, and can also explain why the tropical tropopause is higher, colder, and sharper than the extratropical tropopause. Brewer-Dobson circulation is a key element in explaining the observed features of the tropopause. We will use an idealized GCM to further test this hypothesis.

The second model is a two-layer RCE model with interactive hydrological cycle. This extremely simplified model captures the main features of RCE states very well, and its simplicity helps us better understand the basic physics of RCE. With this model, we find that tropospheric relative humidity hardly changes climate in a broad range of SST from 15^oC to 30^oC, which is exactly the temperature range of current tropics. We want to emphasize that it is an alternative argument, aside from the conventional argument with large-scale circulation, on explaining the unchanged relative humidity with climates people usually assume. The key element of this argument is the coupling between radiation and convection. Once we kill this coupling or use an unrealistic relation between emissivity and water vapor path, we might fail to observe this phenomenon.

For future investigation, we are hoping to combine the two simplified models to better understand how the height of tropopause changes with climate (temperature, humidity, etc.), and going further, large-scale circulation such as lateral transport and mid-latitude eddies will be incorporated in the model as well to form a full picture.

Acknowledgements

I would like to thank Geoff Vallis and Kerry Emanuel for suggesting this wonderful project, for their invaluable guidance, and continuous supervision throughout the summer. I also would like to thank Andy Ingersoll for a lot of insightful discussions. Thanks also to the directors for organizing a smooth program. Last, but certainly not least, I would like to thank all Fellows for a memorable summer.

References

[1] G Vaughan and JD Price. On the relation between total ozone and meteorology. *Quarterly Journal of the Royal Meteorological Society*, 117(502):1281–1298, 1991.

[2] James R Holton, Peter H Haynes, Michael E McIntyre, Anne R Douglass, Richard B Rood, and Leonhard Pfister. Stratosphere-troposphere exchange. *Reviews of Geophysics*, 33(4):403–439, 1995.

[3] LJ Wilcox, BJ Hoskins, and KP Shine. A global blended tropopause based on era data. part i: Climatology. *Quarterly Journal of the Royal Meteorological Society*, 138(664):561–575, 2012.

[4] Geoffrey K Vallis. *Atmospheric and oceanic fluid dynamics: fundamentals and large-scale circulation*. Cambridge University Press, 2006.

[5] Issac M Held. On the height of the tropopause and the static stability of the troposphere. *Journal of the Atmospheric Sciences*, 39(2):412–417, 1982.

[6] Pablo Zurita-Gotor and Geoffrey K Vallis. Determination of extratropical tropopause height in an idealized gray radiation model. *Journal of the Atmospheric Sciences*, 70(7):2272–2292, 2013.

[7] Peter H Stone and John H Carlson. Atmospheric lapse rate regimes and their parameterization. *Journal of the Atmospheric Sciences*, 36(3):415–423, 1979.

[8] II Mokhov and MG Akperov. Tropospheric lapse rate and its relation to surface temperature from reanalysis data. *Izvestiya, Atmospheric and Oceanic Physics*, 42(4):430–438, 2006.

[9] Dargan MW Frierson, Isaac M Held, and Pablo Zurita-Gotor. A gray-radiation aquaplanet moist gcm. part i: Static stability and eddy scale. *Journal of the atmospheric sciences*, 63(10):2548–2566, 2006.

[10] Paul A O'Gorman and Tapio Schneider. The hydrological cycle over a wide range of climates simulated with an idealized gcm. *Journal of Climate*, 21(15):3815–3832, 2008.

[11] Kerry Emanuel, Allison A Wing, and Emmanuel M Vincent. Radiative-convective instability. *Journal of Advances in Modeling Earth Systems*, 6(1):75–90, 2014.

[12] DO Staley and GM Jurica. Flux emissivity tables for water vapor, carbon dioxide and ozone. *Journal of Applied Meteorology*, 9(3):365–372, 1970.

[13] Marat Khairoutdinov and Kerry Emanuel. Rotating radiative-convective equilibrium simulated by a cloud-resolving model. *Journal of Advances in Modeling Earth Systems*, 5(4):816–825, 2013.